

# On the Structure of Np(VI) and Np(VII) Species in Alkaline Solution Studied by EXAFS and Quantum Chemical Methods

Hélène Bolvin,<sup>\*,†</sup> U. Wahlgren,<sup>\*,‡</sup> Henry Moll,<sup>\*,§</sup> Tobias Reich,<sup>§</sup> Gerhard Geipel,<sup>§</sup> Thomas Fanghänel,<sup>§</sup> and Ingmar Grenthe<sup>||</sup>

*Institute of Chemistry, University of Tromsø, N-9037 Tromsø, Norway, Institute of Physics, Stockholm University, S-106 91 Stockholm, Sweden, Institute of Radiochemistry, Forschungszentrum Rossendorf e.V., P.O. Box 510119, D-01314 Dresden, Germany, and Inorganic Chemistry, Department of Chemistry, Royal Institute of Technology (KTH), S-100 44 Stockholm, Sweden*

*Received: April 17, 2001; In Final Form: August 23, 2001*

The bond distances and coordination numbers of the predominant Np(VII) complex in strongly alkaline solution have been determined using EXAFS transmission measurements. The stoichiometry and structure of  $\text{NpO}_4(\text{OH})_2^{3-}$  has been deduced by combining these data with different structure models, mostly determined by using DFT based methods. The experimental and theory based distance  $\text{Np(VII)}-\text{O}_{\text{oxo}}$  is 1.89<sub>4</sub> and 1.90 Å, respectively, whereas the  $\text{Np(VII)}-\text{OH}^-$  distance is 2.32<sub>6</sub> and 2.33 Å, respectively. Theory based geometry and bond distances have been obtained also for other Np(VII) and Np(VI) complexes,  $\text{NpO}_2(\text{OH})_4^-$ ,  $\text{NpO}_4^-$ ,  $\text{NpO}_4(\text{OH})_2^{4-}$ , and  $\text{NpO}_2(\text{OH})_4^{2-}$ ,  $\text{NpO}_4^{2-}$ . The “ $\text{NpO}_6$ ” unit has a square bipyramidal geometry both in  $\text{NpO}_4(\text{OH})_2^{3-/4-}$  and in  $\text{NpO}_2(\text{OH})_4^{1-/2-}$ , albeit with some difference in bond distances. The close similarity in structure indicates that no major rearrangements are necessary on electron transfer between Np(VI) and Np(VII), a possible explanation for the stable and reproducible Np(VII)/Np(VI) redox potential observed in alkaline solution. The structure data indicate that new Np(VII) species may be identified by oxidation of Np(VI) solutions at lower hydroxide concentrations.

## Introduction

U(VI) and Np(VII) compounds are iso-electronic, a fact that makes a comparison between their structure and bonding particularly interesting. The first studies of the chemistry of Np(VII) date back to preparative and solution chemical investigations from 1967;<sup>1</sup> these were followed by the structure determination of several Np(VII) compounds using single-crystal X-ray diffraction.<sup>2</sup> The formal potential of the Np(VII)/Np(VI) redox couple in strongly alkaline solutions was found to depend on the hydroxide ion concentration,<sup>3</sup> as indicated by the half-cell reaction



where the composition of the Np(VII) and Np(VI) species was unknown. Shilov<sup>4</sup> has recently reviewed the redox chemistry of Np(VII) in alkaline solution with emphasis on the constitution of the complexes formed. These data together with information on the structure of the U(VI) complex formed in strongly alkaline solution<sup>5</sup> indicate that the Np(VII) and Np(VI) complexes have the stoichiometry  $\text{NpO}_4(\text{OH})_2^{3-}$  and  $\text{NpO}_2(\text{OH})_4^{2-}$ , respectively. The former complex has been identified in X-ray diffraction studies of  $\text{Co}(\text{NH}_3)_6\text{NpO}_4(\text{OH})_2 \cdot 2\text{H}_2\text{O}$ <sup>2f</sup> and  $\text{Na}_3\text{NpO}_4(\text{OH})_2 \cdot n\text{H}_2\text{O}$ ,<sup>2,b-d</sup> which contain discrete complexes with square bipyramidal geometry; four oxo ligands are located

in the equatorial plane and two OH-groups in apical positions. The square bipyramidal arrangement around Np(VII) is also found in  $\text{LiCo}(\text{NH}_3)_6\text{Np}_2\text{O}_8(\text{OH})_2 \cdot 2\text{H}_2\text{O}$ , where the apical oxygen atoms form bridges linking the bipyramids and forming a chain structure.<sup>2b</sup> Np(VII) is also found in  $\text{MNpO}_4$ ,  $M = \text{K}, \text{Rb}, \text{or Cs}$  with a layer structure<sup>2f</sup> obtained by sharing the four equatorial oxo ligands between adjacent Np(VII) ions. There are two prior studies of the structure and composition of the Np(VII) complex formed in alkaline solution; Clark et al.<sup>6</sup> made the first EXAFS study and suggest that the complex has the composition  $\text{NpO}_2(\text{OH})_4^-$  with square bipyramidal geometry, while Soderholm et al.<sup>7</sup> refuted this claim and suggested the formation of  $\text{NpO}_4(\text{OH})_2^{3-}$ . Both EXAFS experiments have been made using fluorescence detection over a limited  $k$ -space range ( $< 12 \text{ \AA}^{-1}$ ), resulting in fairly large uncertainty in the interpretation of the data, as indicated by the different structures proposed by the two groups.

The redox data indicate that there are two OH groups more in the Np(VII) complex than in the Np(VI) species. However, in experiments of this type, one cannot distinguish between complexes of the same charge but with different water content, for example  $\text{NpO}_2(\text{OH})_6^{3-}$ ,  $\text{NpO}_3(\text{OH})_4^{3-}$ ,  $\text{NpO}_4(\text{OH})_2^{3-}$ , and  $\text{NpO}_5^{3-}$  are all equivalent from the experimental point of view. The constitution of the complex can only be determined by a direct structure determination or by theory. To make a choice between the possible structures, we have made a new set of EXAFS experiments up to  $k = 17 \text{ \AA}^{-1}$  in transmission mode in order to obtain more precise data than in the fluorescence experiments. We have also made a set of quantum chemical calculations using Hartree–Fock (HF) and Density Functional Theory (DFT) on the complexes  $\text{NpO}_4(\text{OH})_2^{3-}$ ,  $\text{NpO}_2(\text{OH})_4^-$ , and  $\text{NpO}_4^-$  containing Np(VII) and on  $\text{NpO}_4(\text{OH})_2^{4-}$ ,

\* To whom correspondence should be addressed.

† Institute of Chemistry, University of Tromsø, on leave from IRSAMC, Université Paul Sabatier, F-31062 Toulouse Cedex 4, France.

‡ Institute of Physics, Stockholm University.

§ Institute of Radiochemistry, Forschungszentrum Rossendorf.

|| Inorganic Chemistry, Department of Chemistry, Royal Institute of Technology.

$\text{NpO}_2(\text{OH})_4^{2-}$ , and  $\text{NpO}_4^{2-}$  containing Np(VI).  $\text{NpO}_2(\text{OH})_4^-$  can be compared to a previous experimental study<sup>5a-c</sup> and theoretical calculations<sup>5b,d</sup> on the iso-electronic complex  $\text{UO}_2(\text{OH})_4^{2-}$ . However, the solution chemical data very clearly indicate that  $\text{NpO}_2(\text{OH})_4^-/\text{NpO}_4^-$  are not present in significant amounts. The two iso-electronic ions  $\text{UO}_4^{2-}$  and  $\text{NpO}_4^-$  are addressed in a separate study;<sup>8</sup> the latter was found to have a stable square planar geometry, whereas  $\text{UO}_4^{2-}$  distorts to a tetrahedral geometry. The reason for this is the much larger stabilization of the oxo-bonds by the f-orbitals in  $\text{NpO}_4^-$ . A comparison of different methods showed that B3LYP results were in good agreement with more sophisticated ab initio methods such as CCSD(T).<sup>8</sup>

In the present study, only Hartree–Fock and DFT methods were used, and the different complexes were studied both in the gas phase and by using a continuum model for the solvent. We have for completeness also studied the linear ions  $\text{NpO}_2^{3+}$  and  $\text{NpO}_2^{2+}$ , belonging to the “yl” type. The theory based bond distances and the experimental EXAFS data were used to select a proper structure model for Np(VII) in alkaline solution.

### Experimental Investigations, Methods and Results

**Sample Preparation and EXAFS Measurements.** We followed in general the description given by Clark et al.<sup>6</sup> when synthesising Np(VII). In a first step Np(VI) was produced by electrochemical oxidation of Np(V) in dilute  $\text{HNO}_3$ . Np(VI) was analyzed spectro-photometrically using the strong absorption band at 1220 nm. A dark brown/red precipitate, presumably  $\text{NpO}_2(\text{OH})_2$ , was obtained by adding NaOH. The precipitate was washed and centrifuged with MILLIQ water several times. The solid is insoluble in 2.5 M NaOH. Ozone was bubbled through a mixture of  $\text{NpO}_2(\text{OH})_2$  and 2.5 M NaOH, resulting in the complete dissolution of the precipitate and the formation of a dark green solution. The ozone, about 2000 mg/h, was obtained by passing dry oxygen with a flow rate of approximately 300 l/h through an ozone generator (Erwin Sander Elektroapparatebau GmbH, Uetze-Eltze, Germany). The oxidation state was checked using UV–vis–NIR spectroscopy. The solution showed the characteristic absorption maxima at 412, 618, and 964 nm,<sup>9a</sup> with no evidence of the absorption bands due to Np(VI), cf. Supporting Information, Fig. S1. We used the absorption bands at 412 and 618 nm and the molar absorption coefficients published in the literature<sup>9a</sup> to determine the Np(VII) concentration, 0.015 M, of the test solution measured at the Rossendorf Beamline (ROBL) at ESRF, Grenoble. There was no difference between the absorption spectra of the test solution measured before and after the EXAFS measurement (Figure S1).

The alkaline Np(VII) solution was hermetically sealed under an  $\text{O}_3$  atmosphere in a polyethylene cuvette of 3 mm diameter. An edge jump of 0.2 across the Np  $L_{III}$  absorption edge was measured. The EXAFS transmission spectra were recorded at room temperature using a water-cooled Si(111) double-crystal monochromator of fixed-exit ( $E = 5\text{--}35$  keV) at ROBL. Four spectra were measured and then averaged. Higher harmonics were rejected using two Pt coated silicon mirrors. More information about the EXAFS measurements can be found in ref 10. An Y foil was used for the energy calibration. The ionization energy of the Np  $L_{III}$  electron,  $E_0$ , was defined as 17 625 eV. The data were treated using the EXAFSPAK software.<sup>11</sup> Theoretical backscattering phase and amplitude functions used in data analysis were calculated using the FEFF8 program.<sup>11</sup> For the final calculations, we used single and multiple scattering (MS) phase and amplitude functions, calculated from 9 atoms in a cluster with a 4.0 Å radius, with coordinates taken

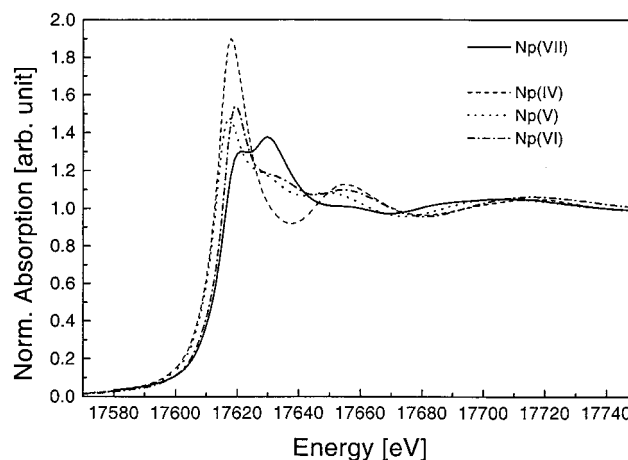


**Figure 1.** Normalized Np  $L_{III}$ -edge XANES spectra of Np solutions. Spectra from Np(IV), Np(V), and Np(VI) were taken from ref. (9b).

**TABLE 1: EXAFS Structural Parameters Measured for Dark-green Np(VII) in 2.5 M NaOH. The X-Ray Diffraction Values within Parenthesis are Taken from Reference (2f)**

sample	shell	$N$	$\sigma^2$ (Å <sup>2</sup> )	$R$ (Å)	residuals	$\Delta E_0$ (eV)
0.015M Np(VII) in 2.5 M NaOH	Np=O	$3.6 \pm 0.3$	0.0020	1.89 <sub>4</sub>	0.18	-5.0
		(4.0)		(1.88 <sub>6</sub> )		
	Np–O	$3.3 \pm 1.3$	0.0133	2.32 <sub>6</sub>		
		(2.0)		(2.32 <sub>3</sub> )		

from the  $\text{Co}(\text{NH}_3)_6\text{NpO}_4(\text{OH})_2 \cdot 2\text{H}_2\text{O}^{2f}$  structure. The amplitude reduction factor,  $S_0^2$ , was held constant at 0.9 for all the fits.

**Results of the EXAFS Measurements.** The X-ray absorption near-edge structure (XANES) of the Np(VII) test solution is given in Figure 1. The pattern is significantly different from that of Np(IV), Np(V), and Np(VI) published in ref 9b. The Np(VII) species shows different symmetry properties, indicating that there is no actinyl unit present like in Np(V) and Np(VI). Soderholm et al.<sup>7</sup> reported a similar XANES spectrum of their Np(VII) sample, whereas the XANES spectrum of Np(VII) in 2.5 M NaOH published by Clark et al.<sup>6</sup> is different. The limited  $k$ -space range and data quality shown in ref 6 makes it difficult to agree with their arguments for the proposed structure model.

The measured bond lengths and coordination numbers for the Np(VII) complex are summarized in Table 1. The EXAFS spectra and corresponding Fourier transforms (FT) are shown in Figure 2. The data indicate a Np–O distance of 1.89 Å, with a Debye–Waller factor, 0.0020 Å<sup>2</sup>. However, the Np–O distance is significantly longer than the “yl” distances found in Np(V) and Np(VI), 1.82 Å, and 1.75 Å, respectively.<sup>9b</sup> The amplitude of the first shell is also larger than that found in “normal” actinyl compounds.<sup>9b</sup> The data from the first shell give  $N = 3.6 \pm 0.3$ , indicating that four oxo ligands are coordinated around Np(VII) in alkaline solution. We continued the analysis with the second shell interactions and found  $N = 3.3 \pm 1.3$  coordinated oxygen atoms at 2.33 Å. The error in  $N$  is large in this case because of the low amplitude and the strong interference from the oxo ligands. A coordination number of 2 for the OH– ligand is in better agreement with the solid-state structure data and the solution chemical data. The bond distance, 2.33 Å, is longer than the U(VI)–OH distance in  $\text{UO}_2(\text{OH})_4^{2-}$  at 2.26 Å, indicating a weaker bonding. As a complex with the constitution  $\text{NpO}_2(\text{OH})_4^-$  is not consistent with the electrochemical observations of Shilov,<sup>4</sup> we conclude that the constitution of Np(VII) in alkaline solution is  $\text{NpO}_4(\text{OH})_2^{3-}$  with a structure as given in Figure 3. This has the same Np(VII) core

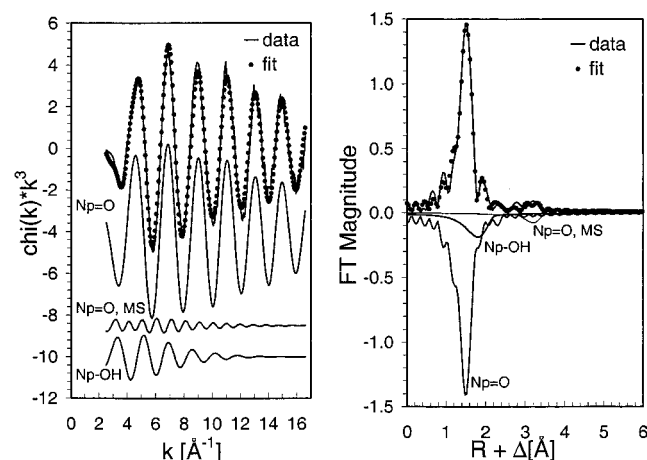


**Figure 2.** Top: Np  $L_{III}$ -edge  $k^3$ -weighted EXAFS data (continuous lines) including the best fit (dotted lines) and corresponding FT's measured for 0.015 M Np(VII) in 2.5 M NaOH. Below: Deconvoluted oscillations resulting from single scattering on the "yl" oxygen atoms (Np=O) and on the oxygen atoms from the OH groups as well as the oscillation from the MS path.

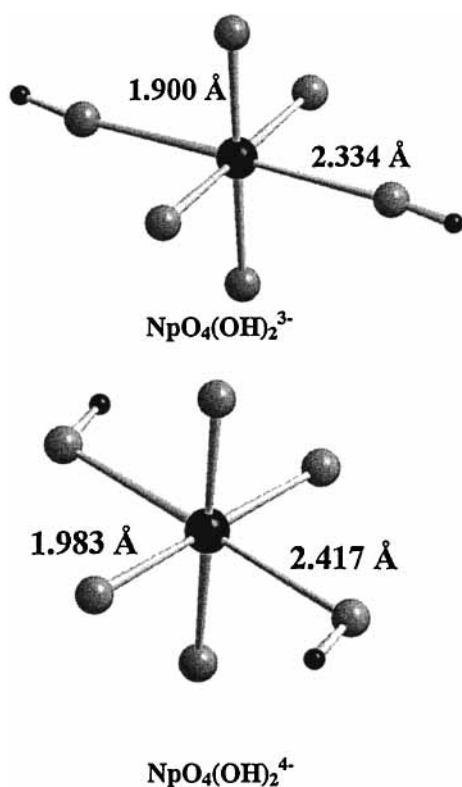


**Figure 3.** Structures of the complexes  $\text{NpO}_4(\text{OH})_2^{3-}$  and  $\text{NpO}_4(\text{OH})_2^{4-}$ . The gray atoms denote oxygen and the small black atom hydrogen. The central atom is Np(VII) and Np(VI), respectively. The geometry has been optimized at the B3LYP level using a CPCM model for the solvent. The bond distances and coordination number for the first structure agrees with the experimental EXAFS results, Np–O 1.894 Å and Np–OH 2.326 Å.

as found in solid-state structures, e.g.,  $\text{Na}_3\text{NpO}_4(\text{OH})_2 \cdot x\text{H}_2\text{O}$ ,<sup>2c</sup> and  $\text{Co}(\text{NH}_3)_6\text{NpO}_4(\text{OH})_2 \cdot 2\text{H}_2\text{O}$ .<sup>2f</sup> The atomic surrounding of Np(VII) measured by EXAFS is in excellent agreement with X-ray diffraction results of these solid structures (see Table 1).

### Computational Details

All calculations have been performed with the energy-consistent relativistic effective core potentials (RECPs) sug-

**TABLE 2: Optimized Bond Distances for the Different Np(VI) and Np(VII) Complexes in  $\text{Å}^a$**

system	model	R(O)HF	B3LYP
$\text{NpO}_3^{3+}$	gas phase	1.60	1.68
$\text{NpO}_2^{3+}$	CPCM	1.60	1.67
$\text{NpO}_2^{2+}$	gas phase	1.64	1.70
$\text{NpO}_2^{2+}$	CPCM	1.66	1.72
$\text{NpO}_4^-$	gas phase	1.79	1.85
$\text{NpO}_4^-$	CPCM	1.83	1.86
$\text{NpO}_4^{2-}$	gas phase	1.79	1.85
$\text{NpO}_4^{2-}$	CPCM	1.91	1.93
$\text{NpO}_2(\text{OH})_4^-$	gas phase	1.69/2.18	1.79/2.18
$\text{NpO}_2(\text{OH})_4^-$	CPCM	1.69/2.18	1.79/2.17
$\text{NpO}_2(\text{OH})_4^{2-}$	gas phase	1.74/2.31	1.83/2.29
$\text{NpO}_2(\text{OH})_4^{2-}$	CPCM	1.74/2.27	1.83/2.25
$\text{UO}_2(\text{OH})_4^{2-}$	gas phase	1.768/2.299 <sup>b</sup>	1.84/2.33 <sup>c</sup>
$\text{NpO}_4(\text{OH})_2^{3-}$	gas phase	dissociative	dissociative
$\text{NpO}_4(\text{OH})_2^{3-}$	CPCM	1.83/2.41	1.90/2.33
$\text{NpO}_4(\text{OH})_2^{4-}$	gas phase	dissociative	dissociative
$\text{NpO}_4(\text{OH})_2^{4-}$	CPCM	1.98/2.40	1.98/2.42

<sup>a</sup> The first distance refers to An–O<sub>oxo</sub>, the second to An–OH<sup>−</sup>. All optimizations have been made without symmetry constraints, the symmetry of the complexes (excluding the hydrogen atom) is close to  $D_{4h}$ .  $\text{NpO}_3^{3+}$  and  $\text{NpO}_2^{2+}$  are linear. The distances obtained using the modified basis set are given in italics, the other with the normal font. The experimentally determined Np–O and Np–OH<sup>−</sup> are 1.89 and 2.32 Å, respectively. <sup>b</sup> from ref 5b in  $D_{2d}$  symmetry. <sup>c</sup> From ref 5d.

gested by the Stuttgart group.<sup>12</sup> For the neptunium atom, the core consists of the 1s–4s, 2p–4p, 3d–4d, and 4f atomic orbitals. Two different basis sets were used to describe the remaining 32 electrons. The first one is the original basis set suggested by the Stuttgart group with 12s 11p 10d 4f contracted to 8s, 7p, 6d, 4f using a partially generalized contraction scheme. Convergence problems encountered in the DFT calculations for some of the negatively charged systems could be removed by modifying the original basis, removing the diffuse s, p, and d functions. In the modified basis set 11s, 10p, 9d, 4f were sequentially contracted to 9s, 8p, 6d, 3f. For the oxygen atoms, the 1s orbital constitutes the core, and the basis set consisted of 4s, 5p, and 1d primitive Gaussians contracted to 2s, 3p, 1d.

All calculations have been performed with the Gaussian 98 program,<sup>13</sup> either at the RHF (Restricted Hartree–Fock), the ROHF (Restricted Open-shell Hartree–Fock) or at the DFT levels using the hybrid functional B3LYP.<sup>14</sup> To describe solvation, we used the Polarizable Continuum Model using the polarizable conductor calculation model CPCM<sup>15</sup> with parameters for water. All geometry optimizations have been done without symmetry constraints. Scalar relativistic effects are taken into account by the ECPs, but we have neglected spin–orbit effects. The latter are in general not important for the ground state of closed-shell system and of minor importance for the structure of actinides complexes with open f-shells.<sup>16</sup>

If not otherwise explicitly stated in the text, all quoted results in the section Results and Discussion are obtained at the B3LYP level.

### Results and Discussion

EXAFS measurements are in general reliable for the determination of bond distances but less precise for the coordination numbers. The experimental and the ab initio results are summarized in Tables 1 and 2, respectively. The Cartesian coordinates and total energies for all species are given in Supplementary Information, Table S1. In the cases where the same species has been optimized with both the original and the modified basis sets, the discrepancy in bond distances and energies is below 0.001 Å and 0.25 kJ, respectively.



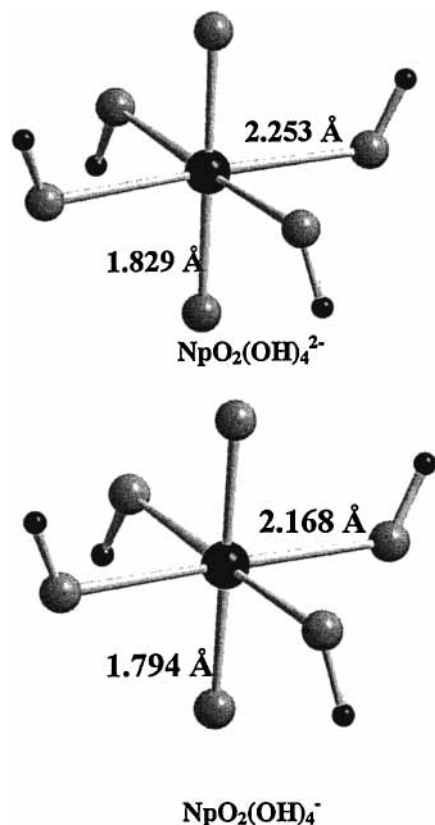


**Figure 4.** Structures of the complexes  $\text{NpO}_2(\text{OH})_4^{2-}$  and  $\text{NpO}_2(\text{OH})_4^-$ . The central atom is Np(VI) and Np(VII), respectively. Both complexes are isostructural with the corresponding U(VI) complex. The gray atoms denote oxide or hydroxide and the small black atom hydrogen. The geometry has been calculated at the B3LYP level using a CPCM model for the solvent.

Perspective drawings of the different structures are shown in Figures 3 and 4.

**Geometry of  $\text{NpO}_2^{3+}$  and  $\text{NpO}_4^-$ .** Previous studies of neptunyl ions include refs 16 and 17 a, b. In the gas-phase  $\text{NpO}_2^{3+}$  is linear and  $\text{NpO}_4^-$  is square planar, with Np(VII)-O bond distances equal to 1.60 and 1.79 Å at the SCF level. At the B3LYP level, the bond distances increase to 1.68 and 1.85 Å, respectively. The accuracy of the B3LYP results were assessed by carrying out explicitly correlated calculations using the CCSD(T) method on  $\text{NpO}_2^{3+}$ . The result, a lengthening of the Np-O bond by 0.09 Å, is in good agreement with the B3LYP result. In ref 17c, d, a bond distance of 1.69 Å, at the B3LYP level, was reported for  $\text{UO}_2^{2+}$ . The difference between  $\text{UO}_2^{2+}$  and  $\text{NpO}_2^{3+}$  is thus fairly small. A somewhat shorter bond distance is expected in  $\text{NpO}_2^{3+}$  than in  $\text{UO}_2^{2+}$  because of the smaller ionic radius of Np(VII) and the larger availability of the 5f orbitals for bonding in neptunium.

The solvent effect at the B3LYP level is negligible for both  $\text{NpO}_2^{3+}$  and  $\text{NpO}_4^-$ , cf. Table 2. The reason for the somewhat larger effect obtained at the SCF level in the latter complex is unclear.

The unpaired electron in the Np(VI) systems occupies an essentially atomic  $f_\phi$  orbital in  $\text{NpO}_2^{2+}$  and an essentially atomic  $f_\delta$  orbital in  $\text{NpO}_4^{2-}$ .

**Geometry of  $\text{NpO}_2(\text{OH})_4^-$  and  $\text{NpO}_2(\text{OH})_4^{2-}$ .** Both ions have a square bi-pyramid structure with two short and four long bonds both in the gas phase and the solvent models, cf. Figure 4. The  $C_1$  structure of  $\text{NpO}_2(\text{OH})_4^-$  is stabilized by 15  $\text{kJ}\cdot\text{mol}^{-1}$  compared to the corresponding  $D_{4h}$  one at the RHF level. The correlation effects on the internal Np-O<sub>oxo</sub> bonds are virtually

the same as in  $\text{NpO}_2^{3+}$  and  $\text{NpO}_2^{2+}$ , (0.1 and 0.07 Å for Np(VII) and Np(VI), compared to 0.07 Å and 0.06 Å without the four hydroxides; all these results are obtained within the CPCM model). This result confirms the assumption made in ref 5b that the correlation effect on the actinyl bond is not sensitive to other ligands. The effect of the solvent is small. In both complexes, the  $\text{OH}^-$  groups are bent out of the plane perpendicular to the “yl” axis with the “trans, 2 up, 2 down” conformer as the ground state. However, the “all up” conformer is only 0.33  $\text{kJ}\cdot\text{mol}^{-1}$  above the ground-state configuration.

$\text{NpO}_2(\text{OH})_4^-$  and  $\text{NpO}_2(\text{OH})_4^{2-}$  are iso-structural with  $\text{UO}_2(\text{OH})_4^{2-}$ .<sup>5a,d</sup> From the results shown in Table 2, we can see that the bonds are significantly shorter in  $\text{NpO}_2(\text{OH})_4^-$  than in  $\text{UO}_2(\text{OH})_4^{2-}$ , whereas they are very similar for  $\text{NpO}_2(\text{OH})_4^{2-}$  and  $\text{UO}_2(\text{OH})_4^{2-}$ . The latter result shows that the single electron in the 5f orbital of Np(VI) is screening the larger charge of the Np nucleus so that the effective nuclear charge of Np(VI) is comparable to U(VI), even though they are not iso-electronic.

The final distances obtained with the solution model are 1.79 Å for the Np-O<sub>oxo</sub> bond and 2.17 Å for the Np-OH bond in the  $\text{NpO}_2(\text{OH})_4^-$  complex. This result does not agree with the experimental results from single-crystal X-ray data or from our EXAFS experiments where these distances are 1.89 and 2.32 Å, indicating that  $\text{NpO}_2(\text{OH})_4^-$  is not the ground state structure.

The unpaired electron in the Np(VI) complex occupies an orbital of  $f_\delta$  character, whereas the open shell in  $\text{NpO}_2^{2+}$  has  $f_\phi$  character. The energy difference between the  $\phi$  and the  $\Delta$  states in  $\text{NpO}_2(\text{OH})_4^{2-}$  is about 0.7 eV at the HF level.

**Geometry of  $\text{NpO}_4(\text{OH})_2^{3-}$  and  $\text{NpO}_4(\text{OH})_2^{4-}$ .** For these systems convergence at the DFT level could only be achieved with a modified basis set as described in the section on computational details.

In the gas-phase both complexes lose their hydroxide ions. However, the solvent stabilizes both complexes to an approximately square bipyramidal configuration with four short Np-O<sub>oxo</sub> and two long Np-OH bonds, cf. Figure 3. The structures of  $\text{NpO}_4(\text{OH})_2^{3-}$  and  $\text{NpO}_4(\text{OH})_2^{4-}$  are very similar cf. Figure 3. The main difference is a shortening of the bond-distances in Np(VII) as compared to Np(VI) and a pronounced change in the Np-O-H angle (107° for Np(VI) and 175° for Np(VII)). There is a decrease in the Np-O<sub>oxo</sub> bond length between the Np(VI) and Np(VII) complexes of about 0.08 Å; the corresponding decrease between  $\text{NpO}_2(\text{OH})_4^-$  and  $\text{NpO}_2(\text{OH})_4^{2-}$  is 0.04 Å.

The final result is Np-O<sub>oxo</sub> and Np-OH distances of 1.90 and 2.33 Å, respectively, in excellent agreement both with single-crystal X-ray and solution EXAFS data, which both give 1.89 and 2.32 Å.

From the EXAFS data we obtained  $3.6 \pm 0.3$  short and  $3.3 \pm 1.3$  long distances. From the good agreement between the theoretical and the experimental bond distances and coordination numbers we conclude that the predominant Np(VII) complex found in solutions with high concentration of  $\text{OH}^-$  is indeed  $\text{NpO}_4(\text{OH})_2^{3-}$ . The large uncertainty in the number of coordinated OH-groups is a result of their small contribution to the EXAFS oscillations, cf. Figure 2.

The recent publication by Williams et al.<sup>19</sup> is based on the same data as reported in ref 7. The Np(VII)-O distances agree well with those reported in our study. However, Williams et al. found a peak at 2.33(3) Å in the *Fourier transformed* data that they assign to the interaction between Np(VII) and 1–2  $\text{Na}^+$ ; this is most likely an experimental artifact because it is not present in our more precise data.

The unpaired electron in  $\text{NpO}_4(\text{OH})_2^{4-}$  occupies an f-orbital of  $\delta$  character, similar to  $\text{NpO}_4^{2-}$ .

**On the Electron Exchange between  $\text{NpO}_4(\text{OH})_2^{3-}$  and  $\text{NpO}_2(\text{OH})_4^{2-}$ .** The redox couple Np(VII)/Np(VI) is reversible in strongly alkaline solution as indicated by the Nernst response between measured potential and concentration. This indicates a rapid electron exchange between the red and the ox forms of the couple at the inert electrode. By just considering the stoichiometry of the complexes, this may seem surprising because changes in stoichiometry and bonding often result in a slow electron exchange and irreversible electrode potentials. The observed reversibility is presumably a result of the similar coordination geometry between  $\text{NpO}_4(\text{OH})_2^{3-}$  and  $\text{NpO}_2(\text{OH})_4^{2-}$ , where the second complex can be looked upon as a protonated form of the first one; proton-transfer reactions and the resulting changes in bond length are often rapid. It would be of interest to explore if such protonation can be experimentally verified, e.g., by oxidizing Np(VI) solutions at lower hydroxide concentrations.

**Acknowledgment.** The XAS experiment was performed at ROBL located at ERSF in Grenoble. The help of C. Henning, S. Pompe, K. Schmeide and H. Funke during the XAS measurements is gratefully acknowledged. Part of this study has been supported by EC under contract FIKW-CT-2000-00035 "ACTAF". H el ene Bolvin was supported by a postdoctoral grant to from the Norwegian Research Council (NFR); this and the support of professor Odd Gropen are gratefully acknowledged. Grants of computing time from the Norwegian Supercomputing Committee (TRU) and a generous grant from the Carl Trygger Foundation are gratefully acknowledged.

**Supporting Information Available:** Table S1 of coordinates in   and total energy in atomic units for the various ions/complexes studied. Figure S1 showing the absorption spectra of Np(VII) in 2.5 M NaOH before and after XAS measurement. For comparison the spectrum of a Np(VI) solution is also given. This material is available free of charge via the Internet at <http://pubs.acs.org>.

## References and Notes

- (1) Krot, N. N.; Gelman, A. D. *Dokl. Akad. Nauk SSSR* **177**, 124.
- (2) (a) Burns, J. H.; Baldwin, W. H.; Stokely, J. R. *Inorg. Chem.* **1973**, *12*, 466. (b) Grigor'ev, M. S.; Glazunov, M. P.; Krot, N. N.; Gavrish, A. A.; Shakh, G. E. *Radiokhimiya* **1979**, *21*, 665. (c) Tomilin, S. V.; Volkov, Y. F.; Kapshukov, I. J.; Rykov, A. J. *Radiokhimiya* **1981**, *23*, 704. (d) *Radiokhimiya* **1981**, *23*, 710. (e) *Radiokhimiya* **1981**, *23*, 862. (f) Grigor'ev, M. S.; Gulev, B. F.; Krot, N. N. *Radiokhimiya* **1986**, *28*, 690.
- (3) (a) Shilov, V. P.; Krot, N. N.; Gel'man, A. D. *Radiokhimiya* **1970**, *12*, 697. (b) Zielen, A. J.; Cohen, D. *J. Phys. Chem.* **1970**, *74*, 394. (c) Ermakov, V. S.; Peretrukhin, V. F.; Krot, N. N. *Radiokhimiya* **1977**, *19*, 72.
- (4) Shilov, V. P. *Radiokhimiya* **1998**, *40*, 12.
- (5) (a) Clark, D. L.; Conradson, S. D.; Donohoe, R. J.; Keogh, D. W.; Morris, D. E.; Palmer, P. D.; Rodgers, R. D.; W., Tait, C. D. *Inorg. Chem.* **1999**, *38*, 1456. (b) Wahlgren, U.; Moll, H.; Grenthe, I.; Schimmelpfennig, B.; Maron, L.; Vallet, V.; Gropen, O. *J. Phys. Chem. A* **1999**, *103*, 1456. (c) Moll, H.; Reich, T.; Szab o, Z. *Radiokhimiya* **2000**, *88*, 411. (d) Schreckenbach, G.; Hay, P. J.; Martin, R. L. *Inorg. Chem.* **1998**, *37*, 4442.
- (6) Clark, D. L.; Conradson, S. D.; Neu, M. P.; Palmer, P. D.; Runde, W.; Tait, C. D. *J. Am. Chem. Soc.* **1997**, *119*, 5259.
- (7) Soderholm, L.; Antonio, M. R.; Williams, C. W.; Sullivan, J. C.; Wasserman, S. R.; Blaudeau, J.-P. *The Redox Speciation of Neptunium in Acidic and Alkaline Solutions*, lecture at the Second Euroconference and NEA Workshop on Speciation, Techniques, and Facilities for Radioactive Materials at Synchrotron Light Sources, Grenoble, France (September 10–12, 2000).
- (8) Bolvin, H.; Wahlgren, U.; Marsden, C.; Gropen, O. *J. Phys. Chem. A* **2001**, *105*, 10570.
- (9) (a) Spitsyn, V. I.; Gelman, A. D.; Krot, N. N.; Mefodiyeva, M. P.; Zakharaova, F. A.; Komkov, Yu. A.; Shilov, V. P.; Smirnova, I. V. *J. Inorg. Nucl. Chem.* **1969**, *31*, 2733. (b) Reich, T.; Bernhard, G.; Geipel, G.; Funke, H.; Hennig, C.; Rossberg, A.; Matz, W.; Schell, N.; Nitsche, H. *Radiokhimiya Acta* **2000**, *88*, 663.
- (10) Matz, W.; Schell, N.; Bernhard, G.; Prokert, F.; Reich, T.; Clau fner, J.; Oehme, W.; Schlenk, R.; Diemel, S.; Funke, H.; Eichhorn, F.; Betzl, M.; Pr ohl, D.; Strauch, U.; H uttig, G.; Krug, H.; Newmann, W.; Brendler, V.; Reichel, P.; Denecke, M. A.; Nitsche, H. *J. Synchrotron Rad.* **1999**, *6*, 1076.
- (11) (a) George, G. N.; Pickering, I. J. 1995. EXAFSPAK, A suite of computer programs for analysis of X-ray absorption spectra. Stanford Synchrotron Radiation Laboratory, Stanford, USA. (b) Ankunidov, A. L.; Ravel, B.; Rehr, J. J.; Conradson, S. D. *Phys. Rev. B* **1998**, *58*, 7565.
- (12) K uchle, W.; Dolg, M.; Stoll, H.; Preuss, H. *J. Phys. Chem. A* **1994**, *100*, 7535.
- (13) Frisch, M. J.; Trucks, G. W.; Schlegel, H. B.; Scuseria, G. E.; Robb, M. A.; Cheeseman, J. R.; Zakrzewski, V. G.; Montgomery, J. A., Jr.; Stratmann, R. E.; Burant, J. C.; Dapprich, S.; Millam, J. M.; Daniels, A. D.; Kudin, K. N.; Strain, M. C.; Farkas, O.; Tomasi, J.; Barone, V.; Cossi, M.; Cammi, R.; Mennucci, B.; Pomelli, C.; Adamo, C.; Clifford, S.; Ochterski, J.; Petersson, G. A.; Ayala, P. Y.; Cui, Q.; Morokuma, K.; Malick, D. K.; Rabuck, A. D.; Raghavachari, K.; Foresman, J. B.; Cioslowski, J.; Ortiz, J. V.; Stefanov, B. B.; Liu, G.; Liashenko, A.; Piskorz, P.; Komaromi, I.; Gomperts, R.; Martin, R. L.; Fox, D. J.; Keith, T.; Al-Laham, M. A.; Peng, C. Y.; Nanayakkara, A.; Gonzalez, C.; Challacombe, M.; Gill, P. M. W.; Johnson, B. G.; Chen, W.; Wong, M. W.; Andres, J. L.; Head-Gordon, M.; Replogle, E. S.; Pople, J. A. *Gaussian 98*, revision A.9; Gaussian, Inc.: Pittsburgh, PA, 1998.
- (14) (a) Becke, A. D. *Phys. Rev. A* **1988**, *38*, 3098. (b) Lee, C.; Yang, W.; Parr, R. G. *Phys. Rev. B* **1988**, *37*, 785. (c) Stevens, P. J.; Devlin, J. F.; Chabalowski, C. F.; Frisch, M. J. *J. Phys. Chem.* **1994**, *98*, 16 123.
- (15) Barone, V.; Cossi, M.; Tomasi, J. *J. Comput. Chem.* **1998**, *19*, 404.
- (16) Vallet, V.; Maron, L.; Schimmelpfennig, B.; Leininger, T.; Teichteil, C.; Gropen, O.; Grenthe, I.; Wahlgren, U. *J. Phys. Chem. A* **1999**, *103*, 9285.
- (17) (a) Wadt, W. R. *J. Am. Chem. Soc.* **1981**, *103*, 6053. (b) Pyykk o, P.; Laakkonen, L. J.; Tatsumi, K. *Inorg. Chem.* **1989**, *28*, 1801. (c) Ismail, N.; Heully, J.-L.; Saue, T.; Daudey, J. P.; Marsden, C. J. *Chem. Phys. Lett.* **1999**, *300*, 296. (d) Vallet, V.; Schimmelpfennig, B.; Maron, L.; Teichteil, C.; Leininger, T.; Gropen, O.; Grenthe, I. and Wahlgren, U. *Chem. Phys.* **1999**, *244*, 185.
- (18) (a) Cornl, H. H.; Heinemann, C.; Marcado, J.; Pores de Matos, A.; Schwartz, H. *Angew. Chem., Int. Ed. Engl.* **1996**, *35*, 891. (b) Jones, L. H. *J. Chem. Phys.* **1955**, *23*, 2105.
- (19) Williams, C. W.; Blaudeau, J.-P.; Sullivan, J. C.; Antonio, M. R.; Bursten, B.; Soderholm, L. *J. Am. Chem. Soc.* **2001**, *123*, 4346.